ACS APPLIED MATERIALS & INTERFACES
Letter
www.acsami.org

Tuning Interfacial Electron Transfer in Nanostructured Cuprous Oxide Photoelectrochemical Cells with Charge-Selective Molecular Coatings

Keith M. Haynes, Kaci C. Kratch, Sean D. Stovall, Christopher O. Obondi, Casey R. Thurber, and W. Justin Youngblood*

Department of Chemistry, University of North Texas, Denton, Texas 76203, United States

Ⓢ *Supporting Information*

ABSTRACT: The coating of nanostructured films of cuprous oxide with electroactive molecules strongly affects their photoelectrochemical performance in nonaqueous photocells, with photocurrent density increased up to an order of magnitude relative to bare cuprous oxide films or almost completely suppressed, depending on the choice of molecular adsorbant. Among adsorbants that enhance photocurrent, a strong variance of photoelectrochemical behavior is observed with changes in the molecular structure of the sensitizer, associated with differences in the reorganization energy and molecular size, which are interpreted to enhance forward electron transport and impede electrolyte/photocathode recombination, respectively. These results demonstrate that nanostructured cuprous oxide is a promising cathode material for p-type dye-sensitized solar cells.

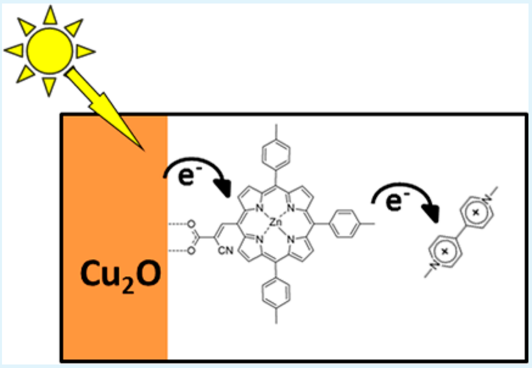

KEYWORDS: *cuprous oxide, molecular coating , solar cells*

Dye-sensitized solar cells (DSCs) employing p-type metal oxide semiconductors, first introduced in 1999 using nickel oxide (NiO) as a mesoporous cathode,[1] are making only slow progress toward rivalling the older and more efficient archetype of DSCs based on wide band gap n-type metal oxide semiconductors such as titanium dioxide. The current record efficiency is at 1.3%,[2] although most reports are well below 0.5%.[3] A significant constraint in the development of p-type DSCs is the identification of a suitable p-type metal oxide photocathode exhibiting good hole mobility and favorable interfacial electron transfer behavior.[3] Pure stoichiometric nickel oxide is alternately described as a Mott-Hubbard insulator or charge-transfer insulator, with a ~4 eV band gap and charge conduction via hole-hopping primarily at defect and/or dopant sites.[4−6] An increase in defect density sufficient to promote hole transport for use as a photocathode material is accomplished through the deliberate preparation of non-stoichiometric NiO via incomplete calcination of nickel hydroxide, resulting in a strongly tinted, often black colloidal cathode for which the absorption of visible light makes no contribution to photocurrent.

There is currently a broad effort to examine replacement photocathode materials that are typically other wide band gap p-type semiconductors, including some delafossites ($CuAlO_2$, $CuGaO_2$, $CuCrO_2$),[7] CuSCN,[8] and spinel-type ternary zinc−cobalt and nickel−cobalt oxides.[9] Far less effort has been invested in the examination of narrow band gap p-type semiconductors, although studies on CuO (also a Mott−Hubbard insulator) and GaAs have been reported.[10,11] Narrow band gap semiconductors allow the possibility of harvesting light energy by the photocathode in tandem with absorption by surface adsorbed dye molecules.

Cuprous oxide (Cu_2O) is a narrow band gap (2.2 eV) semiconductor in the delafossite group of metal oxides.[12] Cu_2O usually exhibits p-type semiconductor behavior due to copper vacancies in the cubic crystal lattice,[13] and has been studied as a photocathode in the light-driven conversion of water to hydrogen as well as in nonaqueous photoelectrochemical cells.[14−17] Difficulties in the preparation of nanostructured Cu_2O make challenging the application of this semiconductor to dye-sensitized solar cells. Sintering a colloid of Cu_2O nanoparticles into a mesoporous film is impractical because Cu_2O oxidizes to CuO at high temperatures (≥300 °C) under ambient atmosphere,[18] or disproportionates to Cu° and CuO at high temperature under vacuum or inert atmosphere.[19,20] Methods for the direct electrochemical preparation of nanostructured Cu_2O have been reported,[18,21] but have not been exploited for the study of molecularly sensitized Cu_2O. We recently reported a templated electrodeposition of Cu_2O using ZnO nanorod films as a sacrificial mold for the in situ preparation of substrate-adhered polymer nanopore membranes.[22] The as-prepared Cu_2O nanorods functioned well in

Received: April 15, 2015
Accepted: June 15, 2015
Published: June 15, 2015

DOI: 10.1021/acsami.5b03094
ACS Appl. Mater. Interfaces 2015, 7, 16133−16137

nonaqueous photoelectrochemical cells employing methyl viologen (MV) as a redox shuttle. Upon examining the coating of Cu_2O nanorod films with dye molecules, we find that the Cu_2O/dye/electrolyte interface exhibits dramatic difference in the balance of forward/back electron transport relative to the bare Cu_2O/electrolyte interface, indicating the operation of an efficient electron transfer cascade (Figure 1). Dye coatings should also offer the possibility of photosensitization of Cu_2O, however this report does not demonstrate that phenomenon because these nanostructured Cu_2O films lack sufficient surface area and translucency to enable significant light absorption a molecular monolayer.

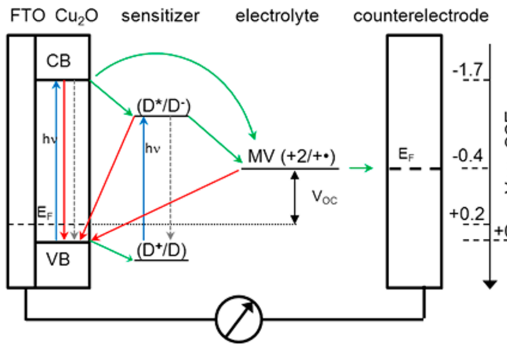

Figure 1. Electron transfer in dye-sensitized Cu_2O solar cells. FTO = F-SnO_2; VB = valence band; CB = conduction band; D = dye; E_F = Fermi level; electrochemical potentials vs saturated calomel electrode are drawn from references.[16,23]

Steady-state electron transfer behavior of molecularly coated Cu_2O films was gauged by assembling them into photoelectrochemical cells prepared with anhydrous acetonitrile electrolyte containing 0.1 M $LiClO_4$ and 50 mM methyl viologen. Decamethylcobaltocene (25 mM) was added to generate a balanced methyl viologen dication/radical cation redox couple. Photoelectrochemical data is shown in Figure 2 and structures of the dyes are shown in Chart 1. Table 1 details the redox potentials of the electroactive adsorbants relative to the conduction and valence band edges of Cu_2O. Three dyes are considered as electron acceptors (**C60M-A**, **NcQ-A**, and PTCDA), and three as electron donors (**ZnP-A**, C343, and N3), although in principle each has a reduction potential positive of the Cu_2O conduction band edge (−1.7 vs SCE)[16] therefore each dye in its neutral state should be capable of accepting a photogenerated electron from Cu_2O. All except PTCDA have reduction potentials that are negative of the methyl viologen redox couple, and oxidation potentials that are positive of the valence band edge (+0.3 vs SCE), and should therefore serve as electron-selective contact layers. With the exception of N3 and PTCDA, the adsorbed dyes had a dramatic

Chart 1. Dyes Used in This Study

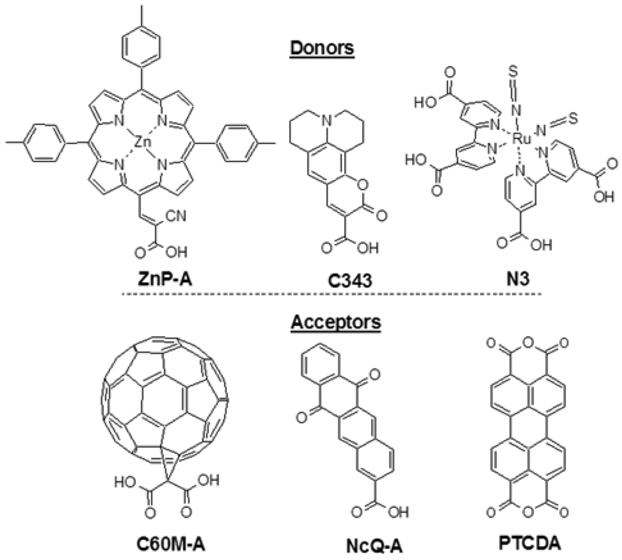

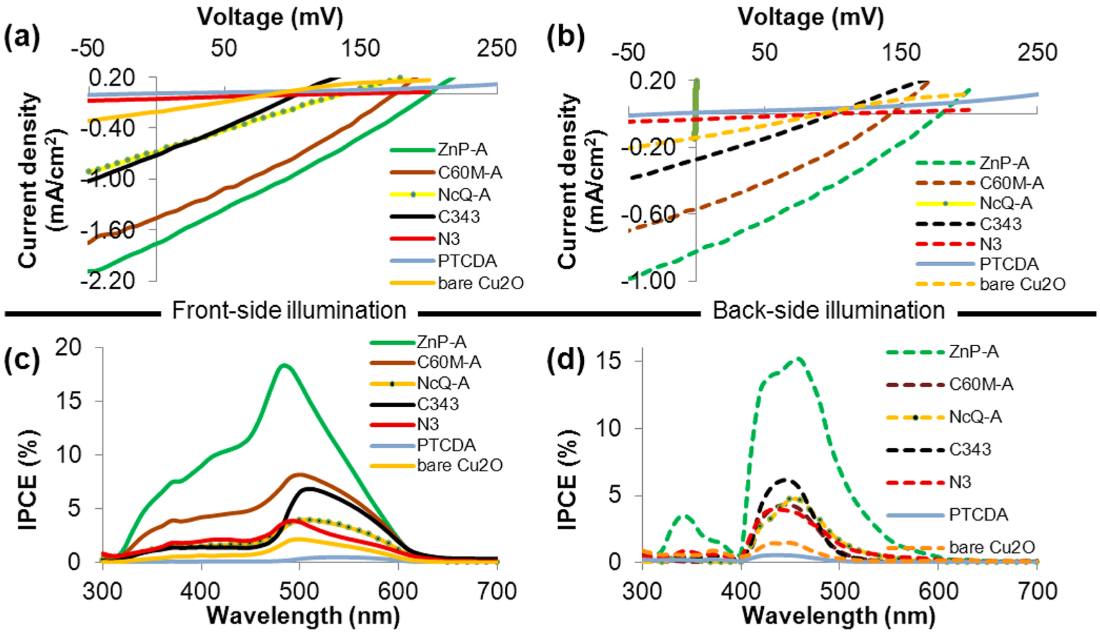

Figure 2. Current−voltage and external quantum efficiency data for photoelectrochemical cells employing bare and molecularly coated Cu_2O photocathodes with methyl viologen redox shuttle. IPCE = incident photons converted to electrons.

Table 1. Redox Potentials of Electroactive Adsorbants and Band Edges of Cu_2O

substance	$RP^{(-)}$/CBE	$OP^{(+)}$/VBE	ref
Cu_2O	−1.74	+0.26	16
N3	−1.40	+0.85	24,25
NcQ	−1.13[a]	+1.75[b]	26,27
ZnP-A	−1.02	+0.85	28
C343	−1.01	+1.39	c
C60-M	−0.64[a]	+0.61	29
MV^{+2}	−0.43		16
PTCDA	−0.29	+2.05	30

All potentials determined for solvated species vs SCE or converted to SCE from other electrodes.[31] RP = reduction potential. CBE = conduction band edge. OP = oxidation potential. VBE = valence band edge. [a]Measured from ester derivative. [b]Reported for 5,12-naphthacenequinone. [c]See Supporting Information.

effect of increasing photocurrent density in the cells (Figure 2). Coating cuprous oxide with 1-adamantanecarboxylic acid, a nonelectroactive molecule, gave impaired photocurrent relative to bare Cu_2O (see the Supporting Information), as did the coatings of N3 and PTCDA, indicating that the nature of the molecular coatings is critical to the enhancement of forward electron transfer at the Cu_2O/electrolyte interface.

For molecularly coated photocathodes, front-side illumination of the cells (at the Cu_2O electrode) gave roughly doubled photocurrent densities compared to back-side illumination, whereas for bare electrodes the difference is marginal and within the limits of device reproducibility (Figure 2a,b and Table S1 in the Supporting Information). Significant optical filtering occurs for illumination in either direction, as shown by the shapes of the IPCE spectra (Figure 2c,d).[22] Back-side illumination is attenuated by photoabsorption of the methyl viologen radical cation. Front-side illumination is attenuated by Cu_2O itself, as photogeneration of carriers far from the oxide surface reduces light transmittance without contribution to photocurrent due to charge recombination. The greater photocurrent densities for front-side illumination indicate that the optical filter effect of the Cu_2O itself has been diminished, meaning that carriers generated at a greater average distance from the surface are harvested before they can recombine within the photocathode. Assuming sufficient driving force, the rate of forward electron transport at the Cu_2O/electrolyte interface is limited by the concentration of electron carriers within the Cu_2O and the concentration of electron acceptors within the electrolyte that are each near the Cu_2O surface. Adsorbed molecules, because of their greater local concentration at the Cu_2O surface, are more efficient than the solution-phase redox couple at harvesting photoexcited electrons from Cu_2O. Thus the electron cascade pathway enhances the forward interfacial electron transport relative to the direct Cu_2O/methyl viologen electron transfer pathway (Figure 1, green arrows). This result also suggests the dye/Cu_2O recombination rate is at least slower than the internal recombination within the oxide. Among the electroactive dyes, PTCDA is the only one with a reduction potential that is positive of the methyl viologen redox couple potential (Table 1). For this sensitizer, thermal electron transfer occurs from the methyl viologen radical cation to the surface-adsorbed molecular monolayer, creating a negatively charged layer at the Cu_2O/electrolyte interface that impedes forward electron transport even up to hundreds of millivolts of forward bias (see the Supporting Information).

IPCE spectra for the molecularly coated photocathodes do not show detectable contribution from the dyes, with the possible exception of **ZnP-A** under front-side illumination (Figure 1c), which shows a shoulder around 430 nm that could corresponding to the porphyrin's Soret band.[32] The weakness of this feature precludes its definitive assignment to the dye. Strong light absorption by the molecular coating requires a very high surface area for the semiconductor film. Treating the Cu_2O nanorods as cylinders of ∼2 μm height and 350 nm diameter, and considering the density of nanorods per unit area through examination of SEM characterization (see the Supporting Information), these nanorod films have just ∼11 times the surface area of a planar film. Visible absorption by the dyes used in this study was not measurable against the background of strong light absorption by the Cu_2O films.

Photovoltages among the molecularly coated Cu_2O photocells track well with photocurrent densities, suggesting that both characteristics are governed by changes in the equilibrium between forward/backward electron transfer events at the semiconductor/electrolyte interface. The trends do not match any progression of known oxidation/reduction potentials of the dyes, as for example, **ZnP-A** has the highest photocurrent and photovoltage but has redox potentials that are intermediary of the other dyes.[24,26,28−30] Factors that should influence the forward and backward electron transport equilibrium include the reorganization energies of the molecular adsorbants and the heights of the monolayers that they form on Cu_2O, respectively. These are shown in Table 2 for all dyes except PTCDA, for which the photoelectrochemical mechanism of its effect can be entirely understood by its relatively positive reduction potential. Low reorganization energies for electron transfer to/from a dye monolayer would aid the forward transport from Cu_2O to the methyl viologen redox shuttle via an electron cascade. Porphyrins and fullerenes have lower reorganization energies than coumarin and quinone compounds. Among the sensitizers, **ZnP-A** would generate the tallest monolayers (19 Å), resulting in significant distance between the redox shuttle and Cu_2O and thereby impeding back electron transfer from the methyl viologen to the photocathode.

Table 2. Inner Sphere Reorganization Energies and Molecular Diameters of Selected Dyes

sensitizer	reorganization energy (eV)	diameter (Å)
ZnP-A	0.14[a]	19
C60M-A	0.06[b]	11
C343	0.2[c]	12
NcQ-A	0.4[d]	15
N3	0.03[e]	11

[a]From ref 33. [b]Value is for C60, from refs 34 and 35. [c]From ref 36. [d]Value is for anthraquinone, from ref 37. [e]from ref 38.

N3-coated Cu_2O shows higher external quantum efficiency than bare Cu_2O in the low intensity light of IPCE characterization (Figure 1c, d); however, the N3-coated photocathode gives a greatly reduced photocurrent density under AM1.5G illumination compared to bare Cu_2O or any other dyes except PTCDA. Cu_2O nanorod films soaked in the N3 staining bath have a pitted appearance with pinholes visible to the naked eye. None of the other dye baths caused the same

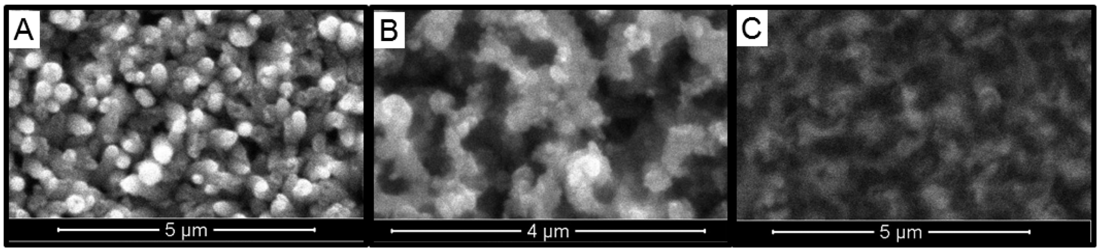

Figure 3. Scanning electron micrograph (SEM) images of dye-soaked Cu_2O nanorod films. (A) Nanorods appear unetched after 24 h of soaking in DMF containing **C60M-A**; (B) significant etching occurs within 6 h of soaking in CH_3CN containing N3; (C) severe etching results from 24 h soaking in the N3/CH_3CN bath.

change in appearance. Scanning electron micrograph (SEM) images of Cu_2O films soaked in the N3 staining bath (in the dark) show significant corrosion of the oxide film (Figure 3). None of the other dye baths caused such corrosion, even after 24 h of soaking. Cu_2O is known to etch in glacial acetic acid and in aqueous mineral acids.[39] Still, we are uncertain as to why the N3 dye causes more rapid etching than other dyes, as all the dye soaking baths were within a narrow range of low concentration (1−3 mM), and the pK_a of isonicotinic acid is higher than that of acetic acid and benzoic acid, and much higher than the acrylic acid binding group of the **ZnP-A**. Further study is needed into the etching of Cu_2O by molecular binding groups. We note that Cu_2O that has corroded during photocatalytic water splitting shows reduced photocurrent,[40,41] and that in at least one instance a ruthenium complex very similar in structure to N3 (Z907 dye) was shown to be unable to photocatalytically transfer electrons via the radical anion state.[42] Either or both of these issues may be involved in the impaired function of the N3-coated Cu_2O photocathodes.

The **ZnP-A**-coated Cu_2O photocell under front side illumination gave a short-circuit current of 1.8 mA/cm^2, an open-circuit voltage of 197 mV, a fill factor of 28%, and an overall efficiency of 0.1%. The attainment of photocurrent densities in the regime of milliamps per square centimeter despite the much lower surface area of these Cu_2O nanorod films compared to mesoporous films of other oxides and the opacity of the methyl viologen electrolyte is a strong indicator that molecularly coated Cu_2O p-type solar cells have great potential to outperform other p-type metal oxide semiconductor in DSCs. Further studies are needed to realize the full potential of dye-coated Cu_2O in nonaqueous photocells. Additional enhancements in photocurrent density will require preparation and coating of films of nanostructured Cu_2O having smaller domain size and greater overall surface area. Dyes that absorb in the red region of the visible spectrum beyond 600 nm would be most suitable for unambiguously characterizing the dye-sensitization of Cu_2O, including via transient spectroscopy studies. Variations in the width of the molecular monolayer would be helpful in exploring control over the Cu_2O/redox couple recombination process; and the identification of other redox couples with greater transparency and more negative redox potential could boost photocurrent and maximum attainable photovoltage, respectively. We hope that these initial results will inspire other researchers interested in the advancement of p-type DSCs to work with Cu_2O.

■ ASSOCIATED CONTENT

Ⓢ Supporting Information

Experimental details, device data for adamantane-coated Cu_2O, cyclic voltammetry of C343, device performance metrics for all photocells, and SEM images of Cu_2O nanorod films before and after dye-soaking. The Supporting Information is available free of charge on the ACS Publications website at DOI: 10.1021/acsami.5b03094.

■ AUTHOR INFORMATION

Corresponding Author

*E-mail: youngblood@unt.edu.

Notes

The authors declare no competing financial interest.

■ ACKNOWLEDGMENTS

We thank the UNT Center for Advanced Research and Technology and Prof. Teresa D. Golden for assistance in obtaining SEM data. We thank Prof. Francis D'Souza assistance in obtaining cyclic voltammetric data.

■ ABBREVIATIONS

DSC, dye-sensitized solar cell
SEM, scanning electron microscopy
IPCE, incident photons converted to electrons

■ REFERENCES

(1) He, J.; Lindstrom, H.; Hagfeldt, A.; Lindquist, S.-E. Dye-Sensitized Nanostructured P-Type Nickel Oxide Film as a Photocathode for a Solar Cell. *J. Phys. Chem. B* **1999**, *103*, 8940−8943.

(2) Powar, S.; Daeneke, T.; Ma, M. T.; Fu, D.; Duffy, N. W.; Götz, G.; Weidelener, M.; Mishra, A.; Bäuerle, P.; Spiccia, L.; Bach, U. Highly Efficient P-Type Dye-Sensitized Solar Cells Based on Tris(1,2-diaminoethane)Cobalt(II)/(III) Electrolytes. *Angew. Chem., Int. Ed.* **2012**, *52*, 602−605.

(3) Odobel, F.; Pellegrin, Y. Recent Advances in the Sensitization of Wide-Band-Gap Nanostructured P-Type Semiconductors. Photovoltaic and Photocatalytic Applications. *J. Phys. Chem. Lett.* **2013**, *4*, 2551−2564.

(4) Gougoussis, C.; Calandra, M.; Seitsonen, A.; Brouder, C.; Shukla, A.; Mauri, F. Intrinsic Charge Transfer Gap in NiO from Ni K-Edge X-Ray Absorption Spectroscopy. *Phys. Rev. B* **2009**, *79*, 045118.

(5) Hufner, S. Electronic Structure of NiO and Related 3d-Transition-Metal Compounds. *Adv. Phys.* **1994**, *43*, 183−356.

(6) Lunkenheimer, P.; Loidl, A.; Ottermann, C. R.; Bange, K. Correlated Barrier Hopping in NiO Films. *Phys. Rev. B* **1991**, *44*, 5927−5930.

(7) Yu, M.; Draskovic, T. I.; Wu, Y. Cu(I)-Based Delafossite Compounds as Photocathodes in P-Type Dye-Sensitized Solar Cells. *Phys. Chem. Chem. Phys.* **2014**, *16*, 5026−5033.

(8) O'Regan, B.; Schwartz, D. T. Efficient Photo-Hole Injection from Adsorbed Cyanine Dyes into Electrodeposited Copper(I) Thiocyanate Thin Films. *Chem. Mater.* **1995**, *7*, 1349−1354.

(9) Mercado, C. C.; Zakutayev, A.; Zhu, K.; Flynn, C. J.; Cahoon, J. F.; Nozik, A. J. Sensitized Zinc-Cobalt-Oxide Spinel P-Type Photoelectrode. *J. Phys. Chem. C* **2014**, *118*, 25340−25349.

(10) Sumikura, S.; Mori, S.; Shimizu, S.; Usami, H.; Suzuki, E. Photoelectrochemical Characteristics of Cells with Dyed and Undyed Nanoporous P-Type Semiconductor CuO Electrodes. *J. Photochem. Photobiol. A: Chem. Chem.* **2008**, *194*, 143−147.

(11) Chitambar, M.; Wang, Z.; Liu, Y.; Rockett, A.; Maldonado, S. Dye-Sensitized Photocathodes: Efficient Light-Stimulated Hole Injection into P-GaP Under Depletion Conditions. *J. Am. Chem. Soc.* **2012**, *134*, 10670−10681.

(12) Assimos, J. A.; Trivich, D. The Photoelectric Threshold, Work Function, and Surface Barrier Potential of Single-Crystal Cuprous Oxide. *Phys. Status Solidi* **1974**, *26*, 477−488.

(13) Raebiger, H.; Lany, S.; Zunger, A. Origins of the P-Type Nature and Cation Deficiency in Cu2O and Related Materials. *Phys. Rev. B* **2007**, *76*, 045209.

(14) Hara, M.; Kondo, T.; Komoda, M.; Ikeda, S.; Shinohara, K.; Tanaka, A.; Kondo, J. N.; Domen, K. Cu2O as a Photoctalyst for Overall Water Splitting Underr Visible Light Irradiation. *Chem. Commun.* **1998**, 357−358.

(15) Paracchino, A.; Brauer, J. C.; Moser, J.-E.; Thimsen, E.; Graetzel, M. Synthesis and Characterization of High-Photoactivity Electrodeposited Cu$_2$O Solar Absorber by Photoelectrochemistry and Ultrafast Spectroscopy. *J. Phys. Chem. C* **2012**, *116*, 7341−7350.

(16) Nagasubramanian, G.; Gioda, A. S.; Bard, A. J. Semiconductor Electrodes XXXVII. Photoelectrochemical Behavior of P-Type Cu$_2$O in Acetonitrile Solutions. *J. Electrochem. Soc.* **1981**, *128*, 2158−2164.

(17) Xiang, C.; Kimball, G. M.; Grimm, R. L.; Brunschwig, B. S.; Atwater, H. A.; Lewis, N. S. 820 mV Open-Circuit Voltages from Cu2O/CH3CN Junctions. *Energy Environ. Sci.* **2011**, *4*, 1311−1318.

(18) Brown, K. E. R.; Choi, K.-S. Electrochemical Synthesis and Characterization of Transparent Nanocrystalline Cu2O Films and Their Conversion to CuO Films. *Chem. Commun.* **2006**, 3311−3313.

(19) Poulston, S.; Parlett, P. M.; Stone, P.; Bowker, M. Surface Oxidation and Reduction of CuO and Cu2O Studied Using XPS and XAES. *Surf. Interface Anal.* **1996**, *24*, 811−820.

(20) Yuhas, B. D.; Yang, P. Nanowire-Based All-Oxide Solar Cells. *J. Am. Chem. Soc.* **2009**, *131*, 3756−3761.

(21) Bijani, S.; Schrebler, R.; Dalchiele, E. A.; Gabás, M.; Martínez, L.; Ramos-Barrado, J. R. Study of the Nucleation and Growth Mechanisms in the Electrodeposition of Micro- and Nanostructured Cu$_2$O Thin Films. *J. Phys. Chem. C* **2011**, *115*, 21373−21382.

(22) Haynes, K. M.; Perry, C. M.; Rivas, M.; Golden, T. D.; Bazan, A.; Quintana, M.; Nesterov, V. N.; Berhe, S. A.; Rodríguez, J.; Estrada, W.; Youngblood, W. J. Templated Electrodeposition and Photocatalytic Activity of Cuprous Oxide Nanorod Arrays. *ACS Appl. Mater. & interfaces* **2015**, *7*, 830−837.

(23) Bockman, T. M.; Kochi, J. K. Isolation and Oxidation-Reduction of Methylviologen Cation Radicals. Novel Disproportionation in Charge-Transfer Salts by X-Ray Crystallography. *J. Org. Chem.* **1990**, *55*, 4127−4135.

(24) Sun, Y.; Onicha, A. C.; Myahkostupov, M.; Castellano, F. N. Viable Alternative to N719 for Dye-Sensitized Solar Cells. *ACS Appl. Mater. Interfaces* **2010**, *2*, 2039−2045.

(25) Nazeeruddin, M. K.; Kay, A.; Rodicio, I.; Humphry-Baker, R.; Müller, E.; Liska, P.; Vlachopoulos, N.; Grätzel, M. Conversion of Light to Electricity by Cis-X2Bis(2,2′-Bipyridyl-4,4′-dicarboxylate)-ruthenium(II) Charge-Transfer Sensitizers (X = Cl-, Br-, I-, CN-, and SCN-) on Nanocrystalline Titanium Dioxide Electrodes. *J. Am. Chem. Soc.* **1993**, *115*.

(26) Roberts, L. W.; Schuster, G. B. Synthesis and Study of Naphthacenedione (TQ) as a Photosensitizer for One-Electron Oxidation of DNA. *Org. Lett.* **2004**, *6*, 3813−3816.

(27) Zweig, A.; Hoffman, A. K.; Maricle, D. L.; Maurer, A. H. An Investigation of the Mechanism of Some Electrochemiluminescent Processes. *J. Am. Chem. Soc.* **1968**, *90*.

(28) Stromberg, J. R.; Marton, A.; Kee, H. L.; Kirmaier, C.; Diers, J. R.; Muthiah, C.; Taniguchi, M.; Lindsey, J. S.; Bocian, D. F.; Meyer, G. J.; Holten, D. Examination of Tethered Porphyrin, Chlorin, and Bacteriochlorin Molecules in Mesoporous Metal-Oxide Solar Cells. *J. Phys. Chem. C* **2007**, *111*.

(29) Guldi, D. M.; Hungerbuhler, H.; Asmus, K.-D. Redox and Excitation Studies with C60-Substituted Malonic Acid Diethyl Esters. *J. Phys. Chem.* **1995**, *99*, 9380−9385.

(30) Slattery, D. K.; Linkous, C. A.; Gruhn, N. E.; Baum, J. C. Semiempirical MO and Voltammetric Estimation of Ionization Potentials of Organic Pigments. Comparison to Gas Phase Ultraviolet Photoelectron Spectroscopy. *Dyes Pigment.* **2001**, *49*, 21−27.

(31) Pavlishchuk, V. V.; Addison, A. W. Converstion Constants for Redox Potentials Measured versus Different Reference Electrodes in Acetonitrile Solutions at 25 °C. *Inorg. Chim. Acta* **2000**, *298*, 97−102.

(32) Muthiah, C.; Taniguchi, M.; Kim, H.-J.; Schmidt, I.; Kee, H. L.; Holten, D.; Bocian, D. F.; Lindsey, J. S. Synthesis and Photophysical Characterization of Porphyrin, Chlorin and Bacteriochlorin Molecules Bearing Tethers for Surface Attachment. *Photochem. Photobiol.* **2007**, *83*.

(33) Jeon, J.; Goddard, W. A.; Kim, H. Inner-Sphere Electron-Transfer Single Iodide Mechanism for Dye Regeneration in Dye-Sensitized Solar Cells. *J. Am. Chem. Soc.* **2013**, *135*, 2431−2434.

(34) Larsson, S.; Klimkans, A.; Rodriguez-Monge, L.; Duškesas, G. Reorganization Energies in Organic Π Systems. *J. Mol. Struct. Theochem* **1998**, *425*, 155−159.

(35) Fukuzumi, S.; Nakanishi, I.; Suenobu, T.; Kadish, K. M. Electron-Transfer Properties of C60 and Tert-Butyl-C60 Radical. *J. Am. Chem. Soc.* **1999**, *121*, 3468−3474.

(36) Kumbhakar, M.; Nath, S.; Mukherjee, T.; Pal, H. Intermolecular Electron Transfer between Coumarin Dyes and Aromatic Amines in Triton-X-100 Micellar Solutions: Evidence for Marcus Inverted Region. *J. Chem. Phys.* **2004**, *120*, 2824−2834.

(37) Rosso, K. M.; Smith, D. M. A.; Wang, Z.; Ainsworth, C. C.; Fredrickson, J. K. Self-Exchange Electron Transfer Kinetics and Reduction Potentials for Anthraquinone Disulfonate. *J. Phys. Chem. A* **2004**, *108*, 3292−3303.

(38) Qu, P.; Meyer, G. J. Proton-Controlled Electron Injection from Molecular Excited States to the Empty States in Nanocrystalline TiO$_2$. *Langmuir* **2001**, *17*, 6720−6728.

(39) Chavez, K. L.; Hess, D. W. A Novel Method of Etching Copper Oxide Using Acetic Acid. *J. Electrochem. Soc.* **2001**, *148*, G640−G643.

(40) Gerischer, H. On The Stability Of Semiconductor Electrodes Against Photodecomposition. *J. Electroanal. Chem.* **1977**, *82*, 133−143.

(41) Wu, L.; Tsui, L.; Swami, N.; Zangari, G. Photoelectrochemical Stability of Electrodeposited Cu2O Films. *J. Phys. Chem. C* **2010**, *114*, 11551−11556.

(42) Wang, P.; Wenger, B.; Humphry-Baker, R.; Moser, J.-E.; Teuscher, J.; Kantlehner, W.; Mezger, J.; Stoyanov, E. V.; Zakeeruddin, S. M.; Grätzel, M. Charge Separation and Efficient Light Energy Conversion in Sensitized Mesoscopic Solar Cells Based on Binary Ionic Liquids. *J. Am. Chem. Soc.* **2005**, *127*, 6850−6856.